ACS APPLIED MATERIALS & INTERFACES

Research Article

www.acsami.org

# Metastable $Ge_{1-x}C_x$ Alloy Nanowires

Byung-Sung Kim,[†,‡] Jae-Hyun Lee,[†,‡] Kiseok Son,[†,‡] Sung Woo Hwang,*[,‡,§] Byoung Lyong Choi,[⊥] Eun Kyung Lee,[⊥] Jong Min Kim,[⊥] and Dongmok Whang*[,†,‡]

[†]Skku Advanced Institute of Nanotechnology, School of Advanced Materials Science and Engineering, Sungkyunkwan University, Suwon 440-746, Korea

[‡]Research Center for Time-domain Nano-functional Devices and [§]School of Electrical Engineering, Korea University, Seoul 136-701, Korea

[⊥]Samsung Advanced Institute of Technology, Yongin, 449-712, Korea.

Supporting Information

**ABSTRACT:** Carbon-containing alloy materials such as $Ge_{1-x}C_x$ are attractive candidates for replacing silicon (Si) in the semiconductor industry. The addition of carbon to diamond lattice not only allows control over the lattice dimensions, but also enhances the electrical properties by enabling variations in strain and compositions. However, extremely low carbon solubility in bulk germanium (Ge) and thermodynamically unfavorable Ge−C bond have hampered the production of crystalline $Ge_{1-x}C_x$ alloy materials in an equilibrium growth system. Here we successfully synthesized high-quality $Ge_{1-x}C_x$ alloy nanowires (NWs) by a nonequilibrium vapor−liquid−solid (VLS) method. The carbon incorporation was controlled by NW growth conditions and the position of carbon atoms in the Ge matrix (at substitutional or interstitial sites) was determined by the carbon concentration. Furthermore, the shrinking of lattice spacing caused by substitutional carbon offered the promising possibility of band gap engineering for photovoltaic and optoelectronic applications.

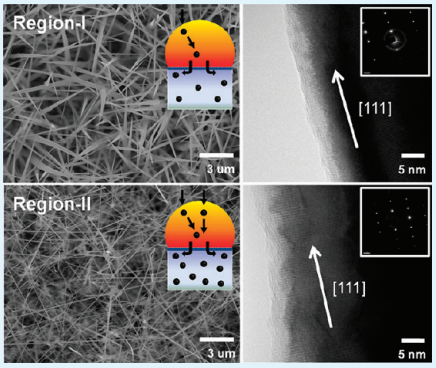


**KEYWORDS:** *germanium−carbon alloy, nanowire, chemical vapor deposition*

## INTRODUCTION

Group IV alloy semiconductors have been studied with great interest because of their potential applications in electronic and optoelectronic devices compatible with silicon (Si)-based technology.[1−4] Carbon-containing alloys such as $Ge_{1-x}C_x$ or $Si_{1-x}C_x$ are of particular scientific and technological interest because strain and band gap can be flexibly controlled by substitutional carbon incorporation into the group IV element matrix.[5−8] In spite of these promising properties, the growth of single crystalline alloy materials is very difficult due to the extremely low equilibrium solubility of carbon in bulk silicon ($1 \times 10^{17}$ $cm^{-3}$) and germanium ($1 \times 10^{8}$ $cm^{-3}$).[9] Nonequilibrium methods such as molecular beam epitaxy (MBE) or rapid thermal chemical vapor deposition (RTCVD) have therefore been used for carbon incorporation above the equilibrium value in bulk alloy systems.[10−13] Compared with bulk materials, the high-quality alloy materials can be synthesized more easily in nanoscale growth systems and several papers have reported incorporation of external atoms with low solubility into IV group semiconductor nanostructures using nonequilibrium growth mode.[14−16]

For high quality of one-dimensional Ge nanostructures, various growth approaches have been developed[17−20] and, especially, the vapor−liquid−solid (VLS) method with a metal catalyst has been widely used for good crystallinity and morphological control.[21] As the source molecules decompose in the vapor phase, they are desorbed into molten metal droplets and diffused across the vapor−liquid interface. When more growth species are supplied, their concentration increases beyond equilibrium in the alloy droplets and supersaturation occurs at the liquid−solid interface.[22] This unique process provides a "non-equilibrium state" to synthesize carbon-containing alloy materials without specific growth systems or organic gases.[23,24] Layer-by-layer growth[25,26] at the interface can also improve homogeneous carbon distribution into the semiconductor matrix, regardless of the thermodynamic instability of the Ge−C bond.

Here we report the synthesis of a single crystalline $Ge_{1-x}C_x$ alloy nanowire (NW) by a VLS-type mechanism with a nonequilibrium solid/liquid interface. The concentration of incorporated carbon and bonding type were controlled in the alloy NW by optimizing growth conditions including temperature and partial pressure of carbon. Furthermore, the reduced lattice constant that depends on the substitutional carbon content indicates the immense potential of Ge-based band gap engineering.

**Received:** October 19, 2011
**Accepted:** December 27, 2011
**Published:** December 27, 2011

  

## EXPERIMENTAL SECTION

**Nanowire Synthesis.** A Si wafer ((100) orientation, B-doped, 0.5−30 Ω cm) with a native oxide layer was chemically cleaned by the standard RCA method followed by the oxygen plasma process to remove organic residues on the surface. Gold (Au) film with a nominal thickness of 2 nm was thermally evaporated on cleaned Si substrates, and the Au-coated Si substrate was subsequently loaded into the low-pressure chemical vapor deposition (LPCVD) system. Single-crystalline $Ge_{1-x}C_x$ alloy NWs were grown by flowing controlled amounts of germane ($GeH_4$), hydrogen chloride (HCl), methane ($CH_4$) and acetylene ($C_2H_2$) gases at temperatures ranging from 300 to 440 °C. To control carbon incorporation, different conditions (region I and region II) with various temperature ($T_g$) and partial pressure of carbon ($P_{CH_4}$ and $P_{C_2H_2}$) were used. Region I conditions were a total pressure of 60 Torr with a fixed partial pressure of $GeH_4$ (10% diluted in $H_2$) and a partial pressure of $CH_4$ (from 3 to 8 Torr) in a temperature range of 300−340 °C. And region II conditions were a total pressure of 40 Torr with a $C_2H_2$ partial pressure (from 8 to 11 Torr) and high temperatures ranging from 400 to 440 °C. Additional HCl gas was introduced to minimize nonspecific Ge deposition at the side walls under region II conditions. The selective use of carbon source gas, $CH_4$ (100%) in region I and $C_2H_2$ (100%) in region II with different decomposition temperatures, supported the controlled growth of metastable $Ge_{1-x}C_x$ alloy NWs.

**Characterization.** SEM images were acquired with a JEOL JSM-7401F field emission scanning electron microscope (FESEM). The crystallinity and composition of the NWs were characterized using a JEOL JEM-2100F transmission electron microscope (TEM) and electron diffraction (ED) analysis. For TEM imaging, $Ge_{1-x}C_x$ alloy NWs suspended in ethanol were dispersed onto a Cu grid with a lacey carbon support film and imaged at an accelerating voltage of 200 kV. Raman spectroscopy (Renishaw, RM-1000 Invia) with excitation energy of 2.41 eV (514 nm, Ar-ion laser) was used to characterize the $Ge_{1-x}C_x$ alloy NWs dispersed on 200 nm Aluminum (Al) substrates. Infrared (IR) absorption measurements in the spectral range of 400−4000 $cm^{-1}$ were performed using an IFS 66 v/s (BRUKER) infrared Fourier-transform spectrometer. The crystal structures of alloy NWs on Si substrates were characterized by X-ray diffraction (XRD, Rigaku D/max-rc). A scanning rate of 0.04/s was applied to record the patterns and data in a $2\theta$ range of 20−100°.

## RESULTS AND DISCUSSION

Considering the extremely low solubility of C in Ge, it is not possible to synthesize high-quality crystalline $Ge_{1-x}C_x$ alloy materials in a general equilibrium-state growth system.[27,28] However, the metal-assisted VLS growth based on a layer-by-layer synthetic mode can provide a nonequilibrium state at the liquid/solid interface, resulting in enhanced homogeneous carbon distribution along the NW elongation. In addition, the chemical vapor deposition (CVD) process allows convenient control of the components of the alloyed NW. A metal catalyst (Au) can act as a window of decomposed carbon species in the vapor phase. Although Au in the bulk state has low carbon solubility, recent research revealed that nanoscale Au particles have significantly increased carbon solubility and can be used with another catalyst for high-quality carbon nanotube growth.[29,30]

Our experimental scheme included two growth parameters, such as temperature and partial pressure of carbon which could critically affect $Ge_{1-x}C_x$ alloy NW formation and controllable carbon incorporation. Also, source gases were selectively used for the controlled supply of carbon. The use of $CH_4$ gas at high temperature has advantage to increase carbon content in alloy NWs because it has lower decomposition temperature than $C_2H_2$ gas. For the successful growth of $Ge_{1-x}C_x$ alloy NWs, a wide range of CVD growth conditions was investigated and the following phenomena were revealed: (i) low temperature ($T_g$ < 400 °C) and high partial pressure ($P_{C_2H_2}$ > 8 Torr) hindered the NW nucleation due to the relatively reduced Ge content and thermal energy; (ii) high temperature ($T_g$ > 400 °C) and low partial pressure ($P_{CH4}$ < 8 Torr) promoted the more active Ge decomposition, resulting a heavily tapered structure with very small carbon concentration; iii) higher temperature ($T_g$ >500 °C) made the incorporated carbon atoms to precipitate on Ge surface at even low partial pressure of carbon. Based on these preliminary studies, the optimized growth conditions for metastable $Ge_{1-x}C_x$ alloy NWs were strategically divided into region I and region II with different carbon source (Figure 1).

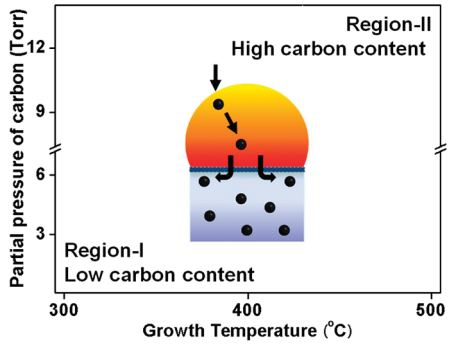


**Figure 1.** Schematic diagram of the strategy used to synthesize $Ge_{1-x}C_x$ alloy NWs with different growth conditions.

Region I conditions were lower partial pressure ($P_{CH_4}$ < 8 Torr) and lower temperature ($T_g$ < 400 °C) for low carbon content, whereas region II conditions were higher partial pressure ($P_{C_2H_2}$ > 8 Torr) and higher temperature ($T_g$ > 400 °C) for high carbon incorporation.

Images a and c in Figure 2 show that high-density $Ge_{1-x}C_x$ alloy NWs were successfully grown under both of region I and region II conditions. Alloy NWs grown under region II conditions (Figure 2c) had less tapered morphology despite high temperatures because additional HCl gas reduced the Ge decomposition at the NW side wall during the growth process.[31,32] Carbon incorporation into the lattice is known to affect the crystallinity of Ge or Si materials.[33] However, high resolution TEM images and clear spots in the diffraction pattern showed that $Ge_{1-x}C_x$ alloy NWs were grown as single crystals without severe deterioration of crystallinity (Figure 2b, d). Also, sharp Ge−Ge peaks at 300 $cm^{-1}$ in the Raman spectra also confirmed that structural disorder did not occur (inset of Figure 2a, c). A selective Ge wet etching process demonstrated that there was no deposition of unwanted carbon atoms on the NW surface and that the Au droplet acted as the exclusive window for carbon incorporation (see Figure S1 in the Supporting Information).

In the $Ge_{1-x}C_x$ alloy system, four different types of chemical bonds (Ge−Ge, Ge−C, $sp^3$ C−C, and $sp^2$ C−C bonds) can be present and can be analyzed by optical measurement tools such as Raman or Fourier transform infrared (FTIR). The Raman spectra for the $Ge_{1-x}C_x$ alloy NWs grown under region I and region II conditions are shown in Figure 3. At low temperature with a $CH_4$ partial pressure of 3 Torr, we did not observe any carbon-related peaks. When the partial pressure was increased under the same conditions, a weak amorphous peak appeared at 1500 $cm^{-1}$ and the intensity gradually increased (Figure 3a).[34] The broad asymmetric peak suggested that incorporated carbon

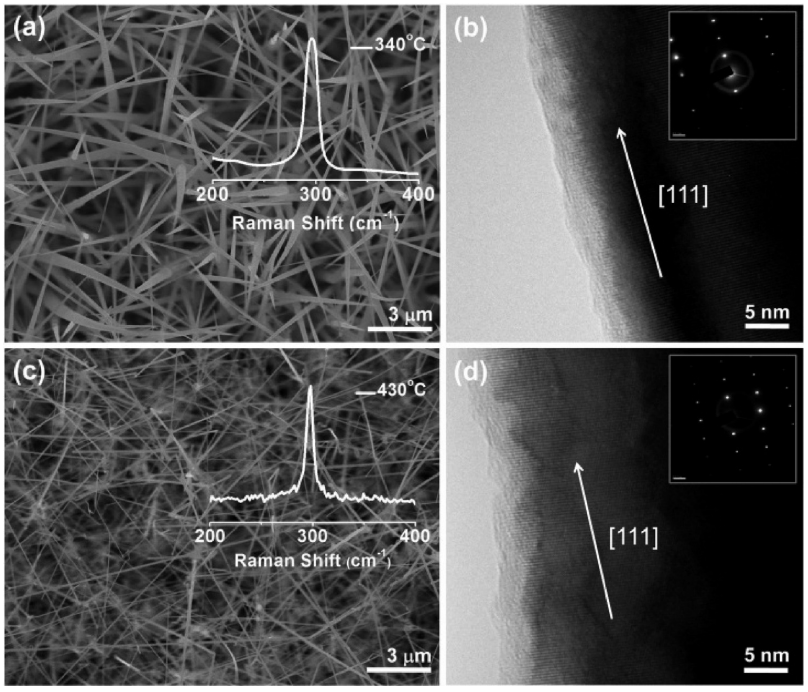


**Figure 2.** Representative SEM and TEM images showing a high density of single crystalline $Ge_{1-x}C_x$ alloy NWs grown at (a, b) 340 °C, $P_{CH_4}$ = 3 Torr and (c, d) 430 °C, $P_{C_2H_2}$ = 11 Torr. The insets are Raman spectra of as-grown alloy NWs dispersed on Al substrates.

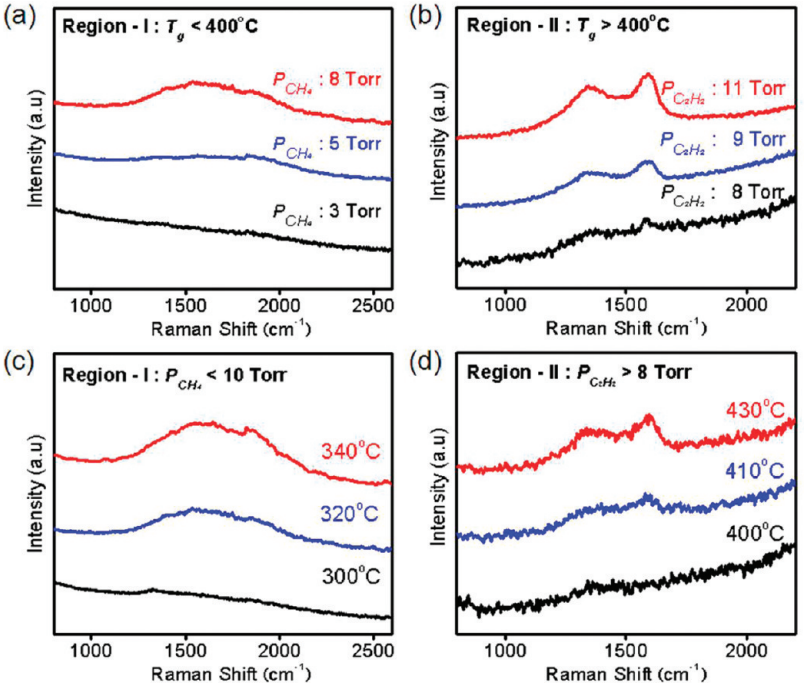


**Figure 3.** (a, b) Raman spectra of $Ge_{1-x}C_x$ alloy NWs as a function of partial pressure at 320 and 430 °C. (c, d) Function of temperature with $CH_4$ and $C_2H_2$ partial pressure of 5 and 8 Torr.

atoms were likely bonded with Ge or with other carbon atoms in $sp^3$ hybridization. However, the peak may have been primarily produced by Ge−C bonds considering the CVD growth conditions of low temperature and partial pressure of carbon.[35,36] Region II conditions with high temperature and partial pressure of carbon invoked active carbon decomposition and sufficient incorporation into the molten metal catalyst. With an increase in the $C_2H_2$ partial pressure from 8 to 11 Torr at 430 °C, two resolved peaks appeared around 1350 and 1550 $cm^{-1}$, corresponding to the D (disorder) and G (graphite) phases of $sp^2$ C−C bonds (Figure 3b).[37,38] This indicates that $sp^2$-bonded multiple configurations of carbon were formed in the alloy NW body and increased depending on the partial pressure of carbon at fixed temperature. A similar tendency was observed when the growth temperature was increased at a fixed partial pressure under region I and region II (Figure 3c, d). It is


dx.doi.org/10.1021/am201446u | ACS Appl. Mater. Interfaces 2012, 4, 805−810

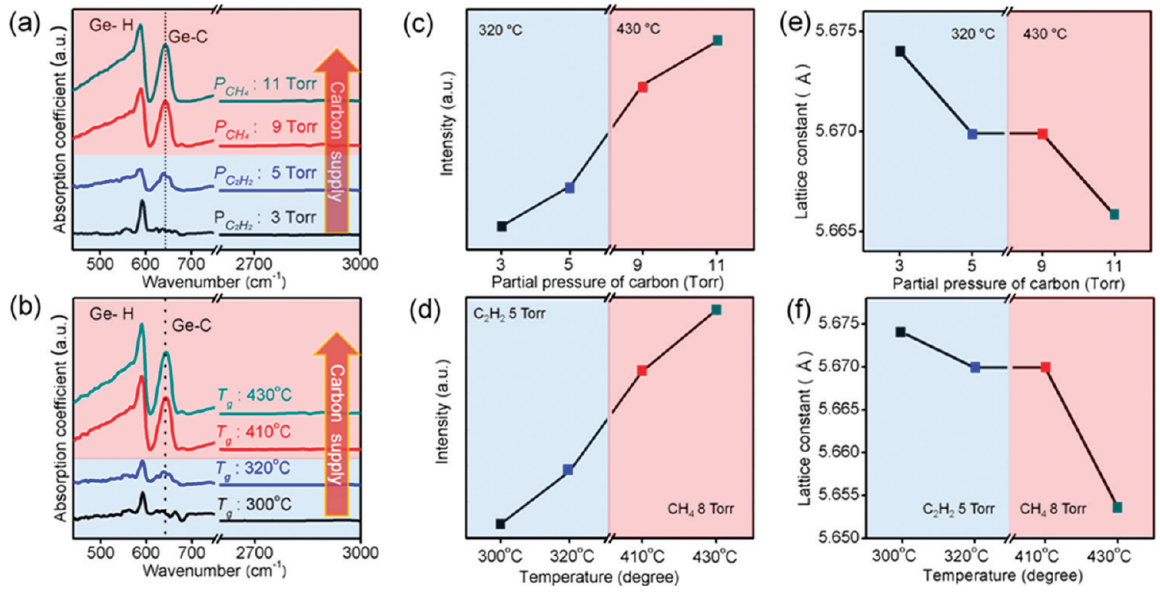


**Figure 4.** (a, b) FTIR absorption spectra for $Ge_{1-x}C_x$ alloy NWs grown under various conditions; region I (blue) $P_{CH_4}$ = 3 and 5 Torr at 320 °C, region II (red) $P_{C_2H_2}$ = 9 and 11 Torr at 430 °C, region I (blue) $P_{CH_4}$ = 5 Torr at 300 and 320 °C, and region II (red) $P_{C_2H_2}$ = 8 Torr at 410 and 430 °C. (c, d) Ge−C peak intensities in FTIR spectra as a function of partial pressure at different temperatures and temperature at different partial pressures of carbon. (e, f) Variation in lattice constants to the growth parameters, as identified by the colored lines in (a, b).

known that when very small amounts of carbon atoms are incorporated into the Ge lattice, they can occupy almost substitutional sites surrounding $sp^3$ hybridized Ge atoms. However, $sp^2$ multiple-carbon configurations are formed in substitutional or interstitial sites as the carbon content increases.[39,40] Contrary to the $Si_{1-x}C_x$ alloy system, the most stable configuration for carbon atoms in the Ge lattice is not the substitutional sites, because the formation energy per carbon atom decreases with increasing numbers of carbon atoms. Theoretical calculation has shown that the formation energy of multiple carbon atoms at a site is lower than for a carbon atom at a substitutional site.[41,42] Therefore, region I conditions with low temperature and partial pressure of carbon induced low carbon decomposition, resulting mainly $sp^3$ bonds to Ge or C atoms. Under region II conditions, $sp^2$ C−C multiple configurations were also formed due to high carbon incorporation in the alloy NW. These results show that not only the carbon concentration but also the configuration in the $Ge_{1-x}C_x$ alloy NW can be controlled by adjusting CVD growth parameters. And, it reveals that region II conditions can induce more carbon incorporation into crystalline $Ge_{1-x}C_x$ alloy NWs than region I ones.

Tunable bandgap energy caused by quantum confinement effect is unique property of nanomaterials and the size reduction to below critical size (e.g., Bohr radius) have shown promising future for optical and electrical application in many papers.[43,44] In addition, the bandgap energy can be controlled by lattice-engineered alloy effect which generates appropriate strain between the mixed atoms. It is known that the incorporated carbon atoms occupy substitutional or interstitial sites in the $Ge_{1-x}C_x$ alloy system, whereas excess atoms are precipitated onto the surface of the material.[45,46] Substitutional carbon atoms reduce lattice spacing of Ge crystal since the very small covalent radii of carbon atoms induce tensile strain associated with lattice spacing. Thus, band gap could be increased with the carbon concentration at substitutional sites. In contrast, interstitial or precipitated carbon atoms result in a decrease of the band gap by increased lattice spacing.[47−50] Panels a and b in Figure 4 show the infrared absorption spectra for $Ge_{1-x}C_x$ alloy NWs grown under region I and region II conditions, according to the temperature or partial pressure of carbon. Two strong absorption bands around 590 and 640 $cm^{-1}$ were clearly visible, and were attributed to the Ge−H wagging and Ge−C vibrations, respectively.[51−53] As the growth temperature and partial pressure of carbon were increased, the intensity of the absorption band corresponding to the Ge−C stretching vibration was increased dramatically (Figure 4c, d). The increase of Ge−C band intensity indicated that the concentration of the substitutional carbon could be controlled by CVD growth parameters.[54,55] The Ge (111) diffraction peak positions of $Ge_{1-x}C_x$ alloy NWs under different growth conditions were carefully evaluated in order to investigate structural change by carbon incorporation (Figure 4e, f). The lattice constant of the alloy NWs was calculated from the XRD pattern and Bragg equation (see Figure S2 in the Supporting Information). With increased partial pressure of carbon or temperature at the other fixed conditions, the lattice constants continued to decrease gradually under the region I and region II. These results clearly demonstrated that relatively many substitutional carbon atoms, as well as interstitial ones, were occupied in Ge matrix and were consistent with the Raman and FTIR analysis in Figures 3 and 4. Considering the region II condition with high temperature and partial pressure, the decrease in lattice constants at region II, compared to those at region I, was relatively small. It can be explained by the formation of $sp^2$ hybridized multiple-carbon configurations in the interstitial sites at region II, compensating for the shrinkage of the lattice dimension by carbon atoms in substitutional sites. On the basis of a theoretical model,[56] we estimate that maximum carbon concentration in $Ge_{1-x}C_x$ alloy NWs is approximately 0.9%. However, the theoretical model assumed that all carbon atoms are substitutional defect and real carbon concentration under region II can be larger than 0.9%


dx.doi.org/10.1021/am201446u | ACS Appl. Mater. Interfaces 2012, 4, 805−810

considering carbon atoms occupied in $sp^2$ interstitial sites in $Ge_{1-x}C_x$ alloy NWs.

The successful synthesis of metastable $Ge_{1-x}C_x$ alloy NWs can be also confirmed by thermal annealing of the alloy NWs since the thermal annealing induces precipitation of incorporated carbon atoms on the surface.[57−59] The Raman spectra of the $Ge_{1-x}C_x$ alloy NW annealed with argon (Ar) gas flow are shown in Figure 5a. We did not observe any other carbon-related Raman peak until an annealing temperature of 500 °C was reached, whereas broad D and G band peaks appeared at 600 °C.

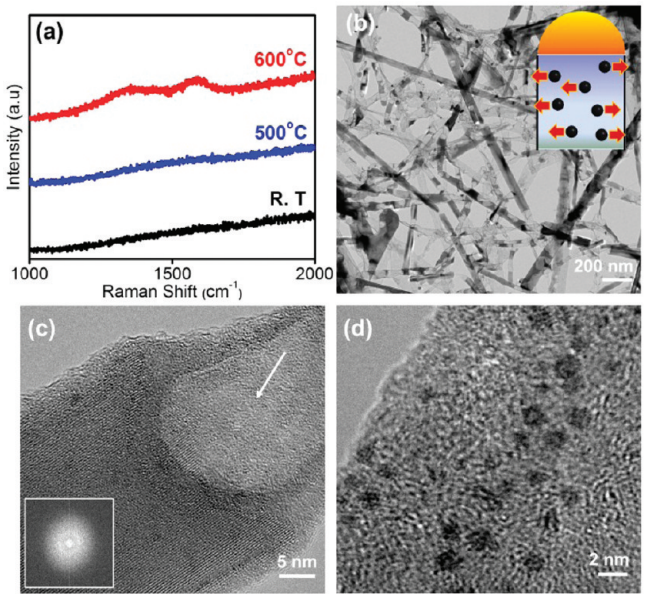


**Figure 5.** (a) Raman spectra showing variations in annealing temperature. (b) TEM image of $Ge_{1-x}C_x$ alloy NWs annealed at 600 °C. The insert shows a simple scheme for the carbon precipitation mechanism. (c) Tubelike NW structure after the annealing process. The diffraction pattern of the insert indicates that only an amorphous carbon shell remained for Ge core vaporization. (d) Magnified TEM image showing that a small carbon cluster formed on the carbon shell.

To investigate the origin of the $sp^2$-related peak, we investigated $Ge_{1-x}C_x$ alloy NWs annealed at 600 °C. In contrast with as-grown alloy NWs, the morphology of annealed NWs was dramatically changed to tubelike structures consisting of a Ge core and carbon shell (Figure 5b). A part of the remaining Ge core still had single crystallinity, whereas another part (white arrow) consisted of only an amorphous carbon shell due to migration and vaporization of Ge (Figure 5c and insert). A magnified image (Figure 5d) showed a small carbon cluster with a 5 nm diameter located in the carbon shell along the NW. The thermal annealing process at high temperature ($T_a$ > 600 °C) provided sufficient thermal energy to carbon atoms in the Ge lattice causing them to diffuse onto the NW surface. Therefore, thermal precipitation of carbon atoms may not only result in the weak D and G band peaks at 600 °C, but may also directly reveal the presence of carbon atoms in metastable $Ge_{1-x}C_x$ alloy NWs.

## CONCLUSION

In summary, we successfully synthesized high-quality single-crystalline $Ge_{1-x}C_x$ alloy NWs in a conventional LPCVD system. A nonequilibrium process at the solid/liquid interface of the VLS mechanism and a metal catalyst as a window can enable incorporation of carbon atoms into the Ge lattice. In addition, we demonstrated that the carbon concentration could be controlled by adjusting growth conditions, and that lattice spacing was reduced by increasing the carbon content in substitutional sites of the Ge diamond lattice, suggesting the promising possibility of band gap engineering of Ge-based material.

## ASSOCIATED CONTENT

### Supporting Information

SEM and XRD of $Ge_{1-x}C_x$ alloy NWs grown with different growth temperatures. This material is available free of charge via the Internet at http://pubs.acs.org.

## AUTHOR INFORMATION

### Corresponding Author

*E-mail: dwhang@skku.edu (D.W.); swhwang@korea.ac.kr (S.W.H).

## ACKNOWLEDGMENTS

This work was supported by the National Research Foundation of Korea (NRF) grant funded by the Korean Government (MEST) (2011-0006268, 2011-0000427).

## REFERENCES

(1) Joshi, G.; Lee, H.; Lan, Y.; Wang, X.; Zhu, G.; Wang, D.; Gould, R. W.; Cuff, D. C.; Tang, M. Y.; Dresselhaus, M. S.; Chen, G.; Ren, Z. *Nano Lett.* **2008**, *8*, 4670−4674.
(2) Lo, Z.; Jiang, R.; Zheng, Y.; Zang, L.; Chen, Z.; Zhu, S.; Cheng, X.; Liu, X. *Appl. Phys. Lett.* **2000**, *77*, 1548−1550.
(3) Pandey, R.; Rérat, M.; Causà, M. *Appl. Phys. Lett.* **1999**, *75*, 4127−4129.
(4) Pascarelli, S.; Boscherini, F.; Mobilio, S.; Zanatta, A. R.; Marques, F. C.; Chambouleyron, I. *Phys. Rev. B* **1992**, *46*, 6718−6723.
(5) Kouvetakis, J.; Nesting, D. C.; Smith, D. J. *ACS Symp. Ser.* **1999**, *727*, 113−129.
(6) Ke, S. H.; Uda, T.; Terakura, K. *Phys. Rev. B* **1999**, *59*, 15013−15018.
(7) Kouvetakis, J.; Nesting, D.; Smith, D. J. *Chem. Mater.* **1998**, *10*, 2935−2949.
(8) Khenata, R.; Baltache, H.; Sahnoun, M.; Driz, M.; Rérat, M.; Abbar, B. *Physica B* **2003**, *336*, 321−328.
(9) Scace, R. I.; Slack, G. A. *J. Chem. Phys.* **1959**, *30*, 1551−1555.
(10) Kolodzey, J.; O'Neil, P. A.; Zhang, S.; Orner, B. A.; Roe, K.; Unruh, K. M.; Swann, C. P.; Waite, M. M.; Shah, S. I. *Appl. Phys. Lett.* **1995**, *67*, 1865.
(11) Okinaka, M.; Hamana, Y.; Tokuda, T.; Ohta, J.; Nunoshita, M. *Physica E* **2003**, *16*, 473−475.
(12) Osten, H. J.; Bugiel, E.; Zaumseil, P. *J. Cryst. Growth* **1994**, *142*, 322−326.
(13) Mi, J.; Warren, P.; Gailhanou, M.; Ganière, J. D.; Dutoit, M.; Jouneau, P. H.; Houriet, R. *J. Vac. Sci. Technol. B* **1996**, *14*, 1660−1669.
(14) Ragan, R.; Ahn, C. C.; Atwater, H. A. *Appl. Phys. Lett.* **2003**, *82*, 3439−3441.
(15) Nakamura, Y.; Masada, A.; Cho, S. P.; Tanaka, N.; Ichikawa, M. *J. Appl. Phys.* **2007**, *102*, 124302.
(16) He, G.; Atwater, H. A. *Phys. Rev. B* **1997**, *79*, 1937−1940.
(17) Wu, Y.; Fan, R.; Yang, P. *Nano Lett.* **2002**, *2*, 83−86.
(18) Dailey, J. W.; Taraci, J.; Clement, I.; Smith, D. J.; Drucker, J.; Picraux, S. T. *J. Appl. Phys.* **2004**, *96*, 7556−7567.
(19) Wu, Y.; Yang, P. *Chem. Mater.* **2000**, *12*, 605−607.
(20) Li, L.; Fang, X.; Chew, H. G.; Zheng, F.; Liew, T. H.; Xu, X.; Zhang, Y.; Pan, S.; Li, G.; Zhang, L. *Adv. Funct. Mater.* **2008**, *18*, 1080−1088.

(21) Wagner, R. S.; Ellis, W. C. *Appl. Phys. Lett.* **1964**, *4*, 89−90.
(22) Schmidt, V.; Wittemann, J. V.; Senz, S.; Gösele, U. *Adv. Mater.* **2009**, *21*, 2681−2702.
(23) Ross, F. M. *Rep. Prog. Phys.* **2010**, *73*, 114501.
(24) Suzuki, M.; Hidaka, Y.; Yanagida, T.; Kanai, M.; Kawai, T.; Kai, S. *Phys. Rev. E* **2010**, *82*, 011605.
(25) Hofmann, S.; Sharma, R.; Wirth, C. T.; Cervantes-Sodi, F.; Ducati, C.; Kasama, T.; Dunin-Borkowski, R. E.; Drucker, J.; Bennett, P.; Robertson, J. *Nat. Mater.* **2008**, *7*, 372−375.
(26) Wen, C. Y.; Reuter, M. C.; Tersoff, J.; Stach, E. A.; Ross, F. M. *Nano Lett.* **2009**, *10*, 514−519.
(27) Eberl, K.; Iyer, S. S.; Zollner, S.; Tsang, J. C.; Legoues, F. K. *Appl. Phys. Lett.* **1992**, *60*, 3033−3035.
(28) Kelires, P. C. *Phys. Rev. B* **1999**, *60*, 10837−10844.
(29) Okamoto, H.; Massalski, T. B. *Bull. Alloy Phase Diagrams* **1984**, *5*, 378−379.
(30) Takagi, D.; Kobayashi, Y.; Hibino, H.; Suzuki, S.; Homma, Y. *Nano Lett.* **2008**, *8*, 832−835.
(31) Kamins, T. I.; Briggs, G. A. D.; Williams, R. S. *Appl. Phys. Lett.* **1998**, *73*, 1862−1864.
(32) Sharma, S.; Kamins, T. I.; Williams, R. S. *J. Cryst. Growth* **2004**, *267*, 613−618.
(33) Ikuta, T.; Fujita, S.; Iwamoto, H.; Kadomura, S.; Shimura, T.; Watanabe, H.; Yasutake, K. *Surf. Interface Anal.* **2008**, *40*, 1122−1125.
(34) Dillon, R. O.; Woollam, J. A.; Katkanant, V. *Phys. Rev. B* **1984**, *29*, 3482−3489.
(35) Chehaidar, A.; Carles, R.; Zwick, A.; Meunier, C.; Cros, B.; Durand, J. *J. Non-Cryst. Solids* **1994**, *169*, 37−46.
(36) Jacobsohn, L. G.; Freire, F. L. Jr; Mariotto, G. *Diamond Relat. Mater.* **1998**, *7*, 440−443.
(37) Ong, S. E.; Zhang, S.; Du, H.; Sun, D. *Diamond Relat. Mater.* **2007**, *16*, 1628−1635.
(38) Ma, T.; Xu, J.; Du, J.; Li, W.; Huang, X.; Chen, K. *J. Appl. Phys.* **2000**, *88*, 6408−6412.
(39) D'Arcy-Gall, J.; Gall, D.; Petrov, I.; Desjardins, P.; Greene, J. E. *J. Appl. Phys.* **2001**, *90*, 3910−3918.
(40) Park, S. Y.; D'Arcy-Gall, J.; Gall, D.; Kim, Y. W.; Desjardins, P.; Greene, J. E. *J. Appl. Phys.* **2002**, *91*, 3644−3652.
(41) D'Arcy-Gall, J.; Gall, D.; Desjardins, P.; Petrov, I.; Greene, J. E. *Phys. Rev. B* **2000**, *62*, 11203−11208.
(42) Gall, D.; D'Arcy-Gall, J.; Greene, J. E. *Phys. Rev. B* **2000**, *62*, R7723.
(43) Nakamura, Y.; Watanabe, K.; Fukuzawa, Y.; Ichikawa, M. *Appl. Phys. Lett.* **2005**, *87*, 1−3.
(44) Musin, R. N.; Wang, X. Q. *Phys. Rev. B.* **2006**, *74*, 165308.
(45) Kanzawa, Y.; Katayama, K.; Nozawa, K.; Saitoh, T.; Kubo, M. *Jpn J. Appl. Phys.* **2001**, *40*, 5880−5884.
(46) Shibata, H.; Kimura, S.; Fons, P.; Yamada, A.; Obara, A.; Kobayashi, N. *Jpn J. Appl. Phys.* **1999**, *38*, 3459−3465.
(47) Hu, C.; Zheng, W.; Tian, H.; Xu, L.; Jiang, Q. *J. Phys.: Condens. Matter* **2006**, *18*, 4231−4241.
(48) Krishnamurthy, M.; Drucker, J. S.; Challa, A. *J. Appl. Phys.* **1995**, *78*, 7070−7073.
(49) Orner, B. A.; Khan, A.; Hits, D.; Chen, F.; Roe, K.; Pickett, J.; Shao, X.; Wilson, R. G.; Berger, P. R.; Kolodzey, J. *J. Electron. Mater.* **1996**, *25*, 297−300.
(50) Yang, B. K.; Krishnamurthy, M.; Weber, W. H. *J. Appl. Phys.* **1997**, *82*, 3287−3296.
(51) Catherine, Y.; Turban, G. *Thin Solid Films* **1980**, *70*, 101−104.
(52) Hu, C. Q.; Zheng, W. T.; Zheng, B.; Li, J. J.; Jin, Z. S.; Bai, X. M.; Tian, H. W.; Jiang, Q.; Wang, X. Y.; Zhu, J. Q.; Meng, S. H.; He, X. D.; Han, J. C. *Vacuum* **2004**, *77*, 63−68.
(53) Vilcarromero, J.; Marques, F. C.; Freire, F. L. Jr *J. Appl. Phys.* **1998**, *84*, 174−180.
(54) Gazicki, M.; Szymanowski, H.; Tyczkowski, J.; Malinovský, L.; Schalko, J.; Fallmann, W. *Thin Solid Films* **1995**, *256*, 31−38.
(55) Saito, N.; Iwata, H.; Nakaaki, I.; Nishioka, K. *Phys. Stat. Sol. (a)* **2009**, *206*, 238−242.
(56) Guedj, C.; Kolodzey, J.; Hairie, A. *Phys. Rev. B* **1999**, *60*, 15150−15153.
(57) Calcagno, L.; Compagnini, G.; Foti, G.; Grimaldi, M. G.; Musumeci, P. *Nucl. Instrum. Methods Phys. Res., Sect. B* **1996**, *120*, 121−124.
(58) Mariotto, G.; Vinegoni, C.; Jacobsohn, L. G.; Freire, F. L. Jr *Diamond Relat. Mater.* **1999**, *8*, 668−672.
(59) Wei, P.; Xu, Y.; Nagata, S.; Narumi, K.; Naramoto, H. *Nucl. Instrum. Methods Phys. Res., Sect. B* **2003**, *206*, 233−236.